

# Concrete structures under severe loading: a strategy to model the response for a large range of dynamic loads

A. Rouquand

*Centre d'Etudes de Gramat (France)*

C. Pontiroli

*Communications & Systems, Merignac (France)*

J. Mazars

*Laboratoire Sols, Solides, Structures - Risques and VOR research network - Grenoble (France)*

**ABSTRACT:** Realistic dynamic description and modelling of material failure is one of the actual problems in structural mechanics. Analyses of failure processes require the use of complex FE analyses and advanced constitutive models. For modeling of concrete it is necessary to capture several important phenomena such as damage and ductility (possibly softening), rate effects ... This implies the description of the concrete behaviour with constitutive equations as refined as possible. In this work a coupled damage and plasticity model including the effective stress concept is used to solve time dependent problems. This is done using an explicit procedure contributing to a reduction of the computational time. Such a procedure requires no iterations and no tangent stiffness matrix. Stability is automatically assured by using small time increments. This strategy has been successfully applied during the last years to model a large range of severe loadings on complex reinforced concrete structures. The main model concepts are presented in this paper and some examples of numerical simulations are given and compared to experimental data.

## 1 INTRODUCTION

The simulation of the failure process in complex reinforced structures is a big challenge. Several physical phenomena must be considered. For example, for high velocity impacts and explosion events near concrete structures, high pressures and high strain rate loading occur locally around the projectile and around the explosive charge. Such phenomena generate pore collapse mechanisms that dissipate a large amount of energy. Irreversible shear strains under high pressure can also be observed driving a significant part of the material response. Under a high pressure regime in porous material, the elastic response becomes non linear and pressure dependent. For soils, rocks and concrete, the water content inside the open voids is very important. This parameter can control the pressure volume relationship and heavily influences the shear material response.

At some distance from the projectile or the explosive charge, the physical phenomena change progressively to become structure oscillations at moderate strain rate levels. The material response is now driven by an increase of concrete damage due to crack opening mechanisms, crack closure effects and friction phenomena related to differential displacements at the crack tip level. The material

model has to account for all of these effects such as stiffness deterioration, recovery of stiffness due to crack closure, or permanent strains and frictional stresses that generate hysteretic loops during unloading and reloading paths. All these mechanisms must be implemented together in a unique material model able to simulate a large range of dynamic problems.

Different kinds of models are proposed to simulate the behaviour of concrete structures including plasticity (Ottosen 1979), damage (Mazars 1986, 1989, Jirasek 2004) or fracture based approaches (Bazant et al. 1996). Nevertheless, very few are able to simulate crash tests (Krieg 1978, Van Mier & al 1991).

The ability of the constitutive model to reproduce the real material behaviour is not the only challenge. Numerical aspects, related to the algorithm used to compute the stress tensor at the local level or related to the computation of structural displacements at the global level in a finite element analysis are also very important. At each level, the computational procedure has to be numerically efficient and robust.

This paper gives some details of the numerical procedure used to perform numerical simulations of concrete structures under severe loadings. Examples are given and finite element results are compared to experimental data.

## 2 DAMAGE AND PLASTIC MODEL FOR CONCRETE : PRM CRASH MODEL

### 2.1 The scalar damage model (PRM model)

#### 2.1.1 Constitutive relations

To simulate the behaviour of concrete at a moderate stress level, a two scalar damage model has been proposed from works by J. Mazars (1986), C. Ponirololi (1995), A. Rouquand (1995 & 2005). The named PRM model simulates the cyclic behaviour of concrete. This model distinguishes the behaviour under tension and the behaviour under compression. Between these two loading states a transition zone is defined by  $(\sigma_{ft}, \varepsilon_{ft})$ . Where  $\sigma_{ft}$  and  $\varepsilon_{ft}$  are respectively the crack closure stress and the crack closure strain. The main equations of the PRM model for a uniaxial loading are :

$$\text{under traction: } (\sigma - \sigma_{ft}) = E_0 \cdot (1-D_t) \cdot (\varepsilon - \varepsilon_{ft})$$

$$\text{under compression: } (\sigma - \sigma_{ft}) = E_0 \cdot (1-D_c) \cdot (\varepsilon - \varepsilon_{ft})$$

$E_0$  is the initial Young's modulus.  $D_t$  evolves as well in tension as in compression through the variable

$$\tilde{\varepsilon} = \sqrt{\sum_i \langle x_i \rangle_+^2} [1], \quad \langle x_i \rangle_+ = x_i \text{ if } x_i > 0 \text{ and } \langle x_i \rangle_+ = 0$$

if not;  $x_i = \varepsilon_i$  are the principal strain components in compression and  $x_i = (\varepsilon - \varepsilon_{ft})_i$  in tension.  $\tilde{\varepsilon}$  is an indicator of the local state of extension (positive strain state), responsible of damage. The general evolution of damage is an exponential form driven by  $\tilde{\varepsilon}$  :  $D_t = \text{fct}(\tilde{\varepsilon}, \varepsilon_{0t}, A_t, B_t)$ ,  $\varepsilon_{0t}$ ,  $A_t$ ,  $B_t$  are material parameters.  $\varepsilon_{0t}$  is the tensile damage threshold.  $D_c$  is driven by the same variable  $\tilde{\varepsilon} = \sqrt{\sum_i \langle \varepsilon_i \rangle_+^2}$  and evolves through the same function:  $D_c = \text{fct}(\tilde{\varepsilon}, \varepsilon_{0c}, A_c, B_c)$ .

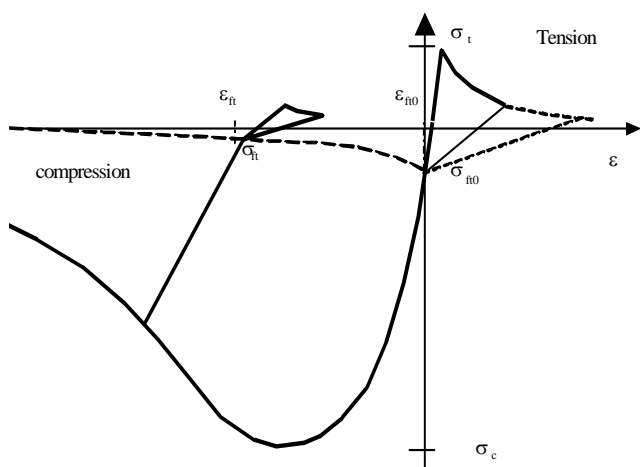


Figure 1. Stress strain curve for a tensile - compressive loading

Initially  $\varepsilon_{ft} = \varepsilon_{ft0}$  is a material parameter. Afterwards  $\varepsilon_{ft}$  is directly link to  $D_c$ .  $\sigma_{ft} = f(\varepsilon_{ft}, D_c)$  gives the stage where the transition between the two kinds of damage occurs. The corresponding response for a uniaxial cyclic loading is given figure 1.

We can observe that the behaviour can be described by the classical equation :  $\sigma_d = E_0 (1-D_i) \varepsilon_d$  with  $i = t, c$ ,  $\varepsilon_d = \varepsilon - \varepsilon_{ft}$  and  $\sigma_d = \sigma - \sigma_{ft}$

The general 3D constitutive equation of the model relating strain and stress tensors (in bold) is reported below :

$$(\boldsymbol{\sigma} - \boldsymbol{\sigma}_{ft}) = \Lambda_0 (1-D) (\boldsymbol{\varepsilon} - \boldsymbol{\varepsilon}_{ft}) \text{ or} \quad (1)$$

$$(\boldsymbol{\sigma} - \boldsymbol{\sigma}_{ft}) = (1-D) [\lambda_0 \text{trace}(\boldsymbol{\varepsilon} - \boldsymbol{\varepsilon}_{ft}) \mathbf{1} + 2\mu_0 (\boldsymbol{\varepsilon} - \boldsymbol{\varepsilon}_{ft})]$$

where  $\boldsymbol{\sigma}_{ft}$  and  $\boldsymbol{\varepsilon}_{ft}$  are the crack closure stress and strain tensors used to manage permanent effects;  $\Lambda_0$  is related to the initial mechanical characteristics of the material.  $D$ , the damage remains a scalar and is issued from a combination of the two modes of damage :

$$D = \alpha_t D_t + (1 - \alpha_t) D_c \quad (2)$$

$\alpha_t$  evolves between 0 and 1 and the actual values depend on  $(\varepsilon - \varepsilon_{ft})$ . For more details see Mazars (1986).

This formulation is an explicit one. It has been implemented into "ABAQUS explicit" and is used for dynamic structural simulations. In order to avoid depending mesh size solutions, a Hillerborg method has been used (Hillerborg 1976) which allows to control the dissipation of energy in each element.

#### 2.1.2 Strain rate effects - Internal friction damping

It is well known that concrete is strain rate dependent particularly by pure tensile loading. This effect is accounted for using dynamic thresholds ( $\varepsilon_{0t}^d$  and  $\varepsilon_{0c}^d$ ) instead of static one's ( $\varepsilon_{0t}^s$  and  $\varepsilon_{0c}^s$ ). Dynamic thresholds are deduced from the static ones through a dynamic increase factor  $R = \varepsilon_{0t}^d / \varepsilon_{0t}^s$ . Its value for a compressive dynamic loading takes the following form:

$$R_c = \min(1.0 + a_c \dot{\varepsilon}^{b_c}, 2.50) \quad (3)$$

And for a dynamic tensile loading :

$$R_t = \min[\max(1.0 + a_t \dot{\varepsilon}^{b_t}, 0.9 \dot{\varepsilon}^{0.46}), 10.0] \quad (4)$$

$a_c$ ,  $b_c$  and  $a_t$ ,  $b_t$  are material coefficients defined by the user. For a high strain rate, the tensile dynamic increase factor is supposed to follow an empirical formula :  $0.9 \dot{\varepsilon}^{0.46}$  that agrees very well with the experimental data obtained by Brara & Klepaczko (1999) on a particular micro concrete. Figure 2 illustrates the evolution of the compressive (dashed

line) and tensile (continuous line) dynamic increase factors versus the strain rate.

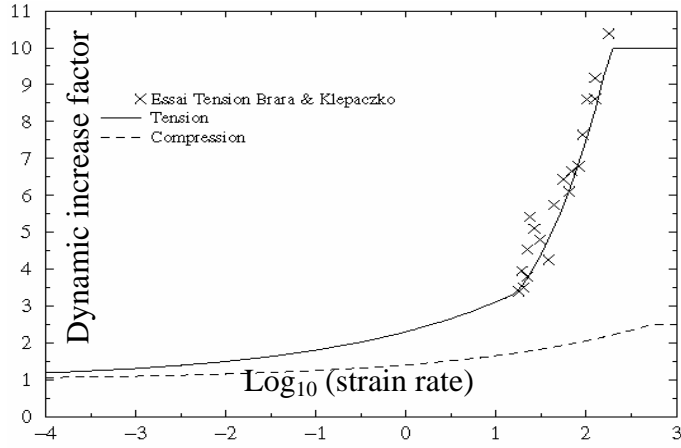


Figure 2. Strain rate effects (PRM damage model).

For cyclic loading, as the one encountered during an earthquake loading, friction stresses induce significant dissipated energy during unloading and reloading cycles. To account for this important phenomenon an additional damping stress is introduced in the model:

$$\underline{\underline{\sigma}} - \underline{\underline{\sigma}}_{ft} = (\underline{\underline{\sigma}} - \underline{\underline{\sigma}}_{ft})^{damage} + \underline{\underline{\sigma}}^{damping} \quad (5)$$

The damping stress generates a hysteretic loop during the unloading and the reloading cycle. This stress is calculated from the damping ratio  $\zeta$  classically defined as the ratio between the area under the closed loop and the area under the linear elastic-damage stress curve :

$$\zeta = \frac{A_h}{E_0(1-D)(\bar{\varepsilon}_{max} - \bar{\varepsilon}_{ft})^2} \quad (6)$$

$A_h$  is the loop area under the stress strain curve,  $E_0(1-D)$  is the current material stiffness.  $\bar{\varepsilon}_{max}$  is the maximum strain before unloading,  $\bar{\varepsilon}_{ft}$  is the closure strain that defines the transition point between compression and tension.

The damping stresses are computed in such a way that the damping ratio  $\zeta$  is related to the damage  $D$  according to the relation :

$$\zeta = (\beta_1 + \beta_2 D) \quad (7)$$

$\beta_1$  is a damping ratio for an undamaged and perfectly elastic material.  $\beta_1 + \beta_2$  is the damping ratio for a fully damaged material.  $\beta_1$  and  $\beta_2$  are material parameters. Usually  $\beta_1$  can be chosen equal to 0.02 and  $\beta_2$  can be chosen equal to 0.05. Figure 3 shows, for cyclic tensile or compressive loading, the strain stress curve including damping stresses.

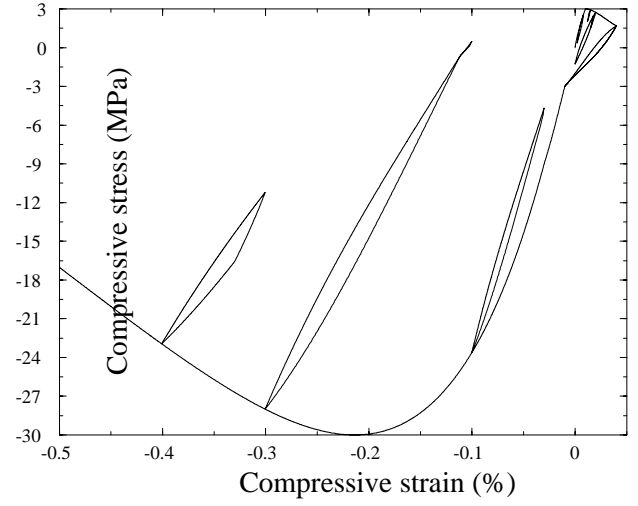


Figure 3. Cyclic loading including damping stresses.

## 2.2 Plastic model with effective stresses

The previous damage model is very efficient to simulate the behaviour of concrete for unconfined or low confined cyclic loading (Rouquand 2005). For very high dynamic loads leading to a higher pressure level, an elastic plastic model is more appropriate. For example, the impact of a projectile striking a concrete plate at 300 m/s induces local pressures near the projectile nozzle of several hundred MPa. The previous damage model cannot simulate the pore collapse phenomena rising at this pressure level. It also cannot model the shear plastic strain occurring in this pressure range. To overcome these limitations, the elastic and plastic model proposed by Krieg (1978) has been chosen to simulate this kind of problem. From this simple elasto-plastic model a first improvement has been introduced in order to simulate the non linear elastic behaviour encountered during an unloading and reloading cycle under a high pressure level. A second improvement has been made to account for the water content effects introducing an effective stress theory as described by C. Mariotti (2002). This effect induces change on the pressure volume curve and on the shear plastic stress limit.

### 2.2.1 The modified Krieg model (dry material)

The Krieg model can be applied to describe the behaviour of a dry material. The improvements made here concern the elastic behaviour which is now non linear and pressure dependent. This non linearity increases as the pore collapse phenomena progresses. Figure 4 shows a typical pressure volume curve used in the modified Krieg model. For pressure values under  $P_1$ , the behaviour between pressure and volume is linear and elastic. For a pressure greater than  $P_1$ , the pore collapse mechanism becomes effective. During the loading process, the pressure-volume response follows a curve identified from experiments. During the unloading, the behaviour is elastic but non linear.

The bulk modulus becomes pressure dependent. It is equal to  $K_{max}$  at the first unloading point and decreases to  $K_{min}$  when the tensile pressure cut-off  $P_{min}$  is reached (this value is generally negative, which means that traction is necessary to recover the initial volume). This pressure cut-off becomes smaller and smaller as the maximum pressure  $P_{max}$  increases. When  $P_{max}$  is close to  $P_I$ ,  $K_{max}$  is close to  $K_{min}$  and also closed to the initial bulk modulus  $K_p$ . When  $P_{max}$  reaches  $P_{cons}$ ,  $K_{max}$  becomes equal to  $K_{grain}$  and  $K_{min}$  becomes equal to  $K_{0grain}$ . So the non linearity becomes more and more important as the pore collapse phenomena progresses.

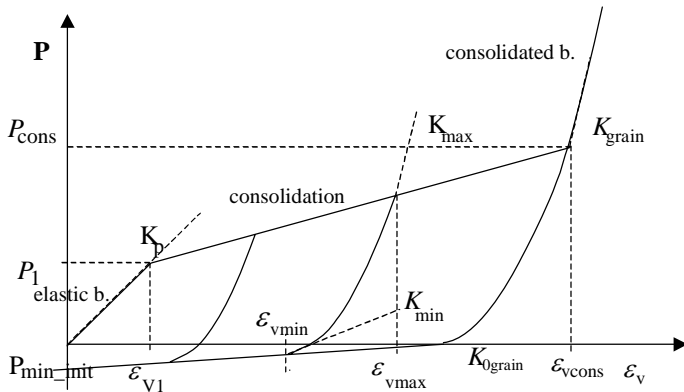


Figure 4. Pressure volume behaviour in the modified elastic and plastic Krieg model.

When  $P_{max}$  becomes greater than  $P_{cons}$ , the pore collapse phenomena is achieved because all the voids are removed from the material. At this pressure level the material is consolidated and the behaviour becomes purely elastic and non linear.

### 2.2.2 Improvement of the Krieg model for partially saturated materials

#### 2.2.2.1 Pressure volume behaviour

Many concrete and geologic media have an open porous structure. The water can move through the porous media from one void to another. Consequently, the void can be partially or totally filled with water. This induces significant changes in the material response and particularly on the relation between pressure and volume.

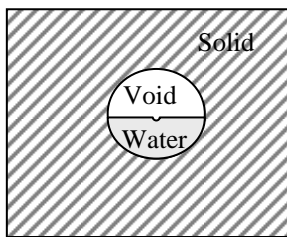


Figure 5: simplified geologic media of a partially saturated material.

To understand more easily the water effect on a geologic medium, the material structure can be

studied as a mixture of a solid medium with a void partially filled with water as shown in figure 5.

For high dynamic loads, the time scale is very low (few milliseconds or less) so the water has no time to move inside the material and undrained conditions can be considered. Figure 6 shows the generic response of a partially saturated material. This response is given in terms of pressure versus the volume change. For a dry material, the pressure volume response follows the solid curve shown on figure 6. When the pressure is sufficient to remove all the voids, the response is given by the thick dashed curve. In case of a partially saturated material, the relation between pressure and volume is given by the response of the dry material until all the voids (part of the pores without water) are removed from the medium. Thereafter, the thin dashed curve gives the response of the solid and water mixture. The intersection of the large dashed curve with the horizontal axis gives the porosity of the dry material. The intersection of the dashed light curve with the horizontal axis gives the “free porosity”  $\epsilon_{vps}$  of the partially saturated material. Consequently, when the material becomes more and more dry, the thin dashed curve moves to the right. In the modified plastic model presented here, the knowledge of the water content ratio  $\eta$  (water volume divided by the total volume) is sufficient to deduce all the improvements of the material behaviour.

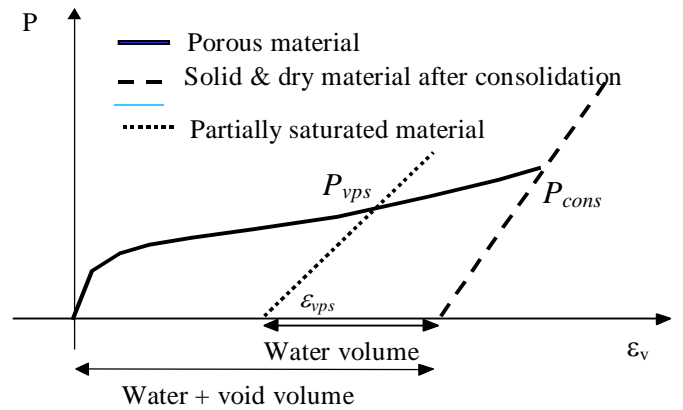


Figure 6. Water content effect on pressure volume relationship

When the pressure reaches the particular value  $P_{vps}$  corresponding to the intersection of the solid line with the thin dashed line, all the voids of the partially saturated medium are removed, so the medium becomes a two phase mixture of liquid and solid. To define the behaviour of this solid and water mixture (thin dashed curve) the pressure is assumed to increase in the same way in the two phases (solid and liquid phases). So an iterative procedure as to be run in order to find the relative volume changes of each phase. This procedure gives a pressure

difference equal to the consolidation pressure of the partially saturated material  $P_{vps}$  when the total volume change of the two phases ( $\varepsilon_v - \varepsilon_{vps}$ ) is known. Liquid behaviour is described using the Mie Gruneisen equation of state and the solid phase behaviour is the non linear elastic model briefly described in § 2.2.1.

#### 2.2.2.2 Shear behaviour

Water content has an effect on the shear behaviour. In the Krieg model, the plastic shear strength  $q_0$  (computed as the Von Mises stress) is pressure dependent (see figure 7). As the pressure increases, the shear yield stress increases too. This effect is the consequence of the porous structure of the material. During the pore collapse phenomena the void volume decreases, the pressure increases so the contact area of the solid grains inside the material matrix increases and the shear forces inducing sliding motions between the solid grains also increase. When all the voids are removed, the shear strength remains constant and becomes pressure independent because the contact area cannot increase any more. The material becomes “homogeneous” and the shear strength reaches a limit that is material dependent. For a partially saturated material, the behaviour remains similar to the behaviour of a dry material until all the voids are removed. Thereafter we suppose that water pressure and solid grain pressure increase together in the same way. So the pressure difference between the two phases remains constant, contact forces and contact areas at the micro scale level maintain constant and the shear strength remains also constant.

At this point, the effective stress concept can be introduced. The shear strength is related to the effective pressure and this effective pressure is taken equal to the interstitial pressure. For a dry material, the effective pressure is always equal to the total pressure. But for a partially saturated material, the effective pressure is the total pressure like in dry material until all the voids are removed. *After consolidation the interstitial (or the effective) pressure does not increase any more and consequently the shear yield strength remains constant.* As the water contents increase, the pressure level  $P_{vps}$  decreases and then the shear strength  $q_0$  also decreases. Figure 7 illustrates the effect of the effective pressure concept. The solid line gives the shear yield strength versus the pressure for a dry material. For a partially saturated one, the shear strength follows the solid line until the pressure  $P_{vps}$  is reached. Afterwards the shear strength does not increase and it follows the dashed horizontal line.

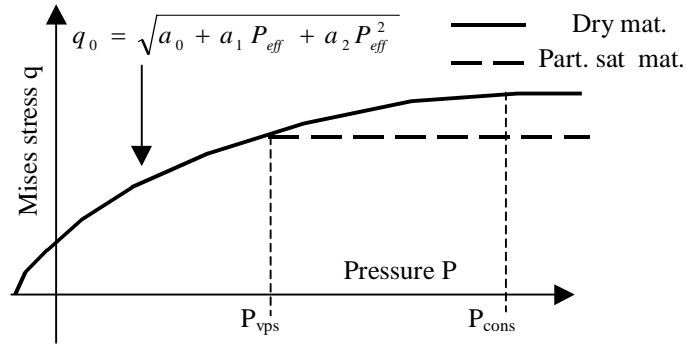


Figure 7. Shear yield strength versus pressure for a dry and a partially saturated material ( $q$  is the Von Mises stress).

### 2.3 Coupling procedure for the damage and the modified Krieg model : PRM crash model

The scalar damage model has been coupled with the modified Krieg model. The coupling procedure ensures a perfect continuity between the two model responses. The predicted stresses correspond to the damage model response if the maximum pressure is too low to start the pore collapse phenomena or if the shear stress is too low to reach the shear yield stress. If not, the plastic model is activated and pilots the evolutions until the extensions sufficiently increase to lead to a damage failure.

Figure 8 shows the static response obtained on a cylindrical specimen for tri-axial tests with increasing lateral pressure. Tests performed on the GIGA machine at 3S-R Grenoble prove the pertinence of these results (Gabet 2006).

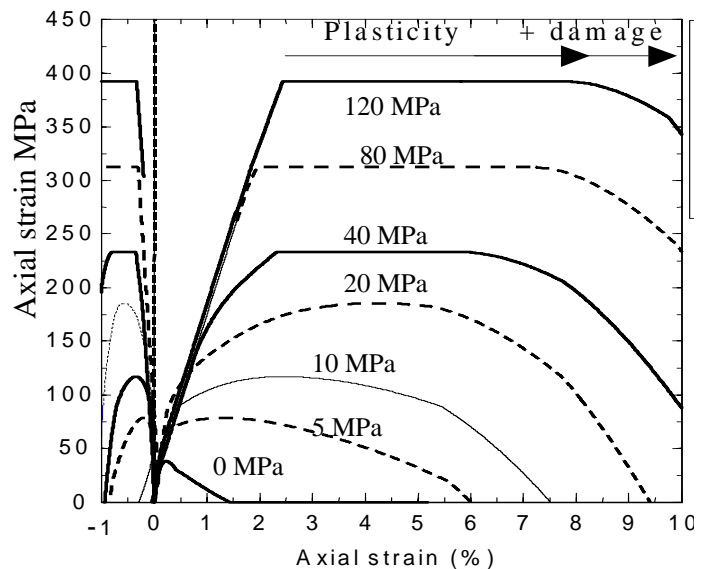


Figure 8. Stress strain response on a concrete given by the coupled damage and plastic model (tri-axial tests with increasing lateral pressure).

### 3 NUMERICAL SIMULATIONS

This model has been implemented in the ABAQUS explicit finite element code and it has been extensively used to simulate a lot of complex problems. The PRM damage model can be used with most of the available finite elements (1D truss elements, beam elements, 2D plane stress and plane strain elements, 2D axisymmetric elements, shell elements, 3D solid elements, etc.). The coupled damage and plastic model (PRM crash model) can be used with 2D plane strain elements, 2D axisymmetric and 3D solid elements. In order to show the capabilities of the coupled model some applications are presented here and numerical results are compared to experimental data.

#### 3.1 Dynamic three points bending test on a reinforced concrete beam

Figure 9 shows the experimental device and the beam characteristics (in mm). These tests have been conducted by Agardh, Magnusson & Hanson (1999) in Sweden on a high strength reinforced concrete beam.

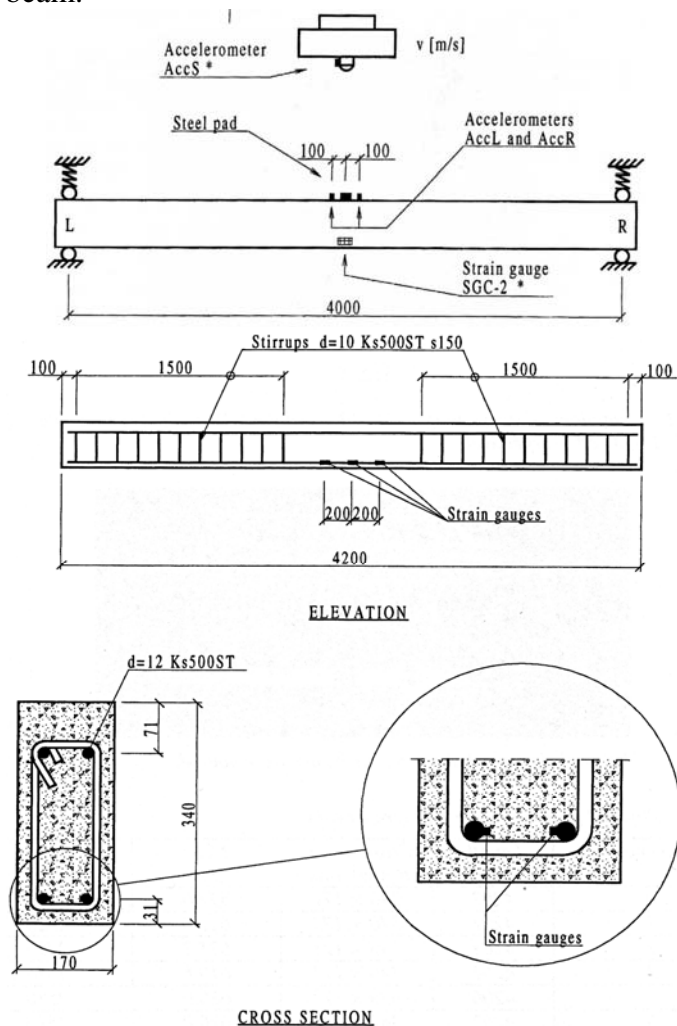


Figure 9. Experimental device and beam characteristics (dynamic three points bending tests).

Beam elements, 2D plane stress elements and 3D solid elements are used to model the reinforced concrete beam. A single element is used in the depth direction with the 3D model. Taking advantage of the symmetry, only a half part of the beam is modelled. The reinforcement material model is the classical Johnson Cook plasticity model. The concrete and the steel reinforcement are supposed to be perfectly bonded. Figure 9 details the experimental apparatus. When the deflection becomes greater than 90 mm, shock absorbers damp the central part of the beam.

Figure 10 shows, at the end of the dynamic test, the tensile damage contours on the 3D beam model (upper part of the figure). The lower part shows the corresponding observed crack pattern. The computed cracks are mainly concentrated in the central part of beam like in the experiment.

In figure 11 the measured force (cross points) is compared to the three computed forces resulting from the three different meshes. The beam model gives the lower force. The 2D and 3D models give very similar results.

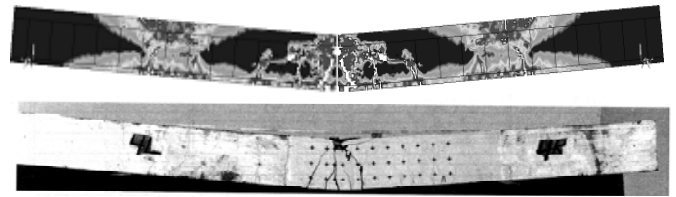


Figure 10. Computed and observed crack pattern.

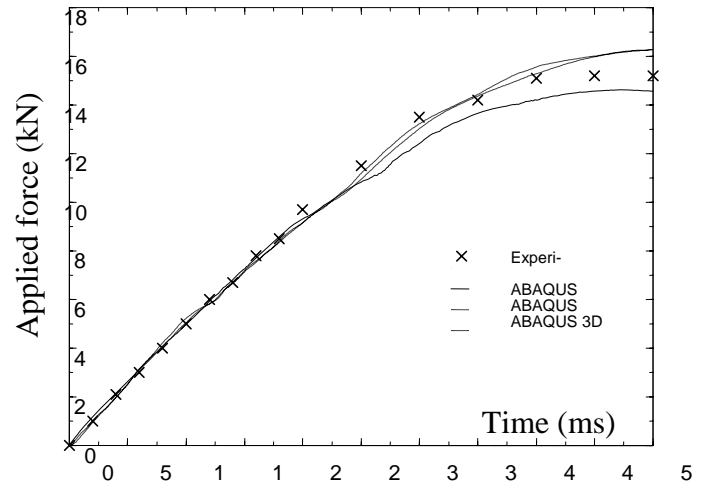


Figure 11. Measured and computed dynamic loads (three points bending test).

#### 3.2 Impact on a T shape reinforced concrete structure

This study is related to the analysis of the vulnerability of concrete structures under intentional actions. More specifically, the effect of a projectile of about 80 kg striking a reinforced concrete plate is studied. Such an experiment has been done by E.

Buzaud et al. (2003). The 35NCD16 steel projectile has an ogival nozzle. Its diameter is 160 mm and its length is 960 mm (figure 13). An accelerometer recorder system is mounted inside the projectile to measure the axial and lateral accelerations during the tests. Figure 12 shows the test configuration with a T shape concrete structure. The size of each reinforced concrete square plate composing the target is 3m. The thickness of the front part of the concrete target is 400 mm and the thickness of the rear part is 300 mm. Reinforcement is composed of two steel layers (one on each side of the concrete plate) with 16 mm diameter bars. Other 10 mm diameter bars link each reinforcement mesh node of the face to face layers. The distance that separates each bar is 100 mm. The distance between the reinforcement layer and the top (or the bottom) plate surface is 50 mm.

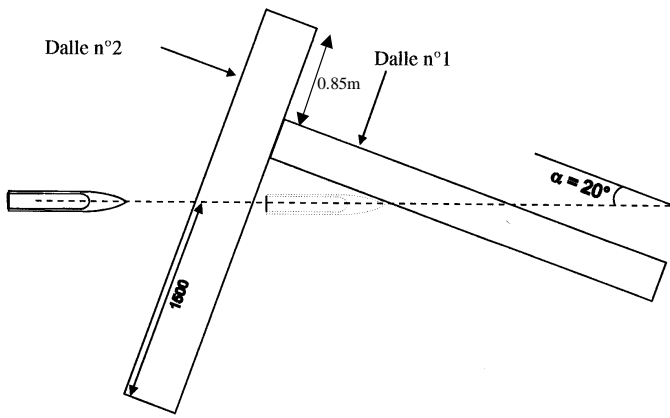


Figure 12. Test configuration, impact on T structure.

3D numerical simulations have been done using the ABAQUS explicit finite element code. The total number of the finite elements is about 530 000 for the entire model. The projectile material (figure 13) is simulated using an elastic and perfectly plastic model with a plastic yield stress of 1300 MPa. The reinforcement is also modelled with an elasto-plastic model with isotropic hardening. The initial yield stress is 600 MPa and reaches 633 MPa for a failure strain  $\epsilon = 0.13$ . The concrete behaviour is simulated with the coupled plastic and damage model.

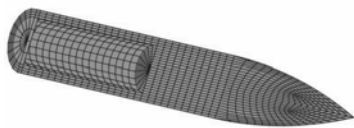


Figure 13. Projectile mesh.

Table 1 gives the concrete material data used in the simulation. Most of these values are taken from literature data relative to similar materials. On figure 14, the measured deceleration is compared to the computed value. Some differences can be seen

but the overall deceleration shape is correctly predicted.

Table 1. Concrete material data

Sym-bol	Parameter	Value S.I. units
$E_0$	Young modulus	$3.5 \cdot 10^{10}$
$\nu_0$	Poisson ratio	0.2
$\sigma_c$	Compressive strength	$-41 \cdot 10^6$
$\sigma_t$	Tensile strength	$3.3 \cdot 10^6$
$G_f$	Fracture energy	120
$a_0$	1 <sup>st</sup> coefficient (shear strength)	$1.8 \cdot 10^{15}$
$a_1$	2 <sup>nd</sup> coefficient (shear strength)	$2.4 \cdot 10^8$
$a_2$	3 <sup>rd</sup> coefficient (shear strength)	0.6
$n$	N <sup>o</sup> of points (compaction curve)	2
$P_1$	Pressure	$60 \cdot 10^6$
$\epsilon_{v1}$	Volume	-0.00308
$P_{cons}$	Consolidation pressure (last point)	$2 \cdot 10^9$
$\epsilon_{vcons}$	Corresponding volume (last point)	-0.1284
$K_{grain}$	Bulk modulus at consolidation	$3.9 \cdot 10^{10}$
$K_{0grain}$	Bulk modulus unloaded material	$3.9 \cdot 10^9$
$\eta_{eau}$	Water contents ratio	0
$\rho_0$	Density	2300

Figure 15 shows the tensile damage contours at the end of the numerical simulation ( $T = 20$  ms). The first part of the target is perforated and a rebound off the rear part is observed. This has been observed experimentally. The projectile velocity, at the exit of the first impacted plate, is also close to the measured one.

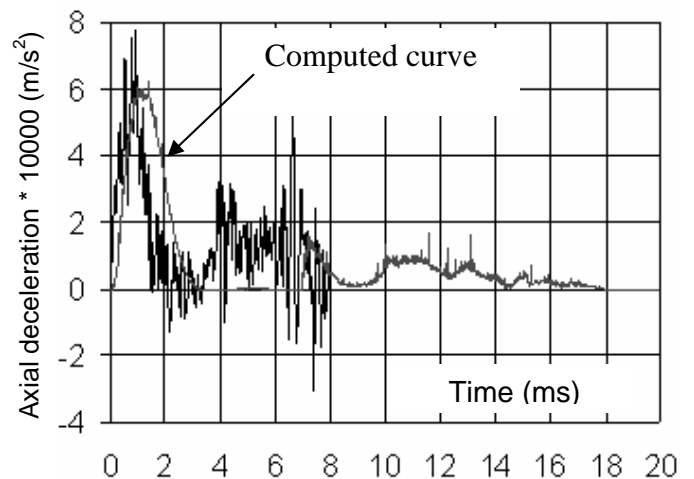


Figure 14. Measured and computed projectile decelerations.

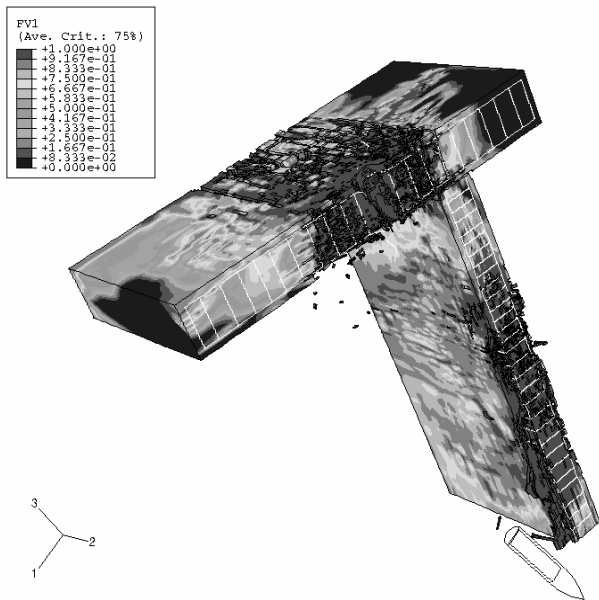


Figure 15. Tensile damage contours at 20 ms. The projectile has perforated the upper part and penetrated the right part after a rebound.

#### 4 CONCLUSION

A general constitutive model for a concrete structure submitted to extreme loading (high velocity and high confinement) has been developed and implemented into the “ABAQUS explicit” code in the framework of damage and plasticity mechanics. The resulting coupled damage and plasticity model (*PRM crash model*) can simulate a lot of physical mechanisms like crack opening and crack closure effects, strain rate effects, material damping induced by internal friction, compaction of porous media, shear plastic strains under high pressure, water content effects on the pressure volume behaviour and on the shear strength.

To validate this particular coupling of plasticity and damage, an extensive experimental program has been performed at 3S-R Grenoble using the GIGA machine which allows high confinement up to 1 GPa (Gabet 2006), and a new program is in progress on the large Hopkinson bar at JRC Ispra to complete the data base under high velocity loading.

The new model has been extensively used and can advantageously simulate a large panel of problems going from quasi-static simulations on concrete structures to high dynamic problems related to the effect of high velocity impacts.

The examples presented here and during the conference, demonstrate the efficiency of the proposed numerical procedure.

#### REFERENCES

- Agardh L., Magnusson J., Hansson H., 1999, High strength concrete beams subjected to impact loading, an experimental study, FOA Defence Research Establishment, FOA-R-99-01187-311—SE.
- Bazant Z.P., 1994, “Nonlocal damage theory based on micro-mechanics of crack interaction”. *Journal Engineering Mech.* ASCE 120, pp. 593-617.
- Brara A., 1999, Etude expérimentale de la traction dynamique du béton par écaillage, *thèse de l'université de Metz - France*
- Buzaud E. et al., 2003, An experimental investigation of corner effects resulting from vertical attack on hardened structures, *proceedings of 11<sup>th</sup> ISIEMS*, Mannheim, Germany.
- Gabet T., 2006, Comportement triaxial du béton sous fortes contraintes : Influence du trajet de chargement, Phd thesis, Université Joseph Fourier, Grenoble.
- Hillerborg A., Modeer M., Petersson P. E., 1976, Analysis of crack formation and growth in concrete beams of fracture mechanics and finite elements, *Cement and Concrete Research*, Vol. 6, pp 773-782.
- Jirásek M., 2004, “Non-local damage mechanics with application to concrete”. *Revue française de génie civil*, 8 (2004), pp. 683-707.
- Krieg R. D., 1978, A simple constitutive description for soils and crushable foams, Sandia National Laboratories, SC-DR-72-0833, Albuquerque, New Mexico.
- Mariotti C., Perlat J. P., Guerin J. M., 2002, A numerical approach for partially saturated geomaterials under shock, CEA/DAM Bruyères le Châtel, *International Journal of Impact Engineering* 28 (2003) 717 - 741.
- Mazars J., 1986. A description of micro and macro scale damage of concrete structures, *Engineering Fracture Mechanics*, V. 25, n° 5/6.
- Mazars J., Pijaudier-Cabot G., 1989, “Continuum damage theory - application to concrete. *Journal of Engineering Mechanics*”. 115(2), pp. 345–365.
- Ottosen N.S., 1979, “Constitutive model for short time loading of concrete”. *Journal of Engineering Mechanics*, ASCE, Vol 105, pp. 127-141.
- Rouquand A., Pontiroli C., 1995, Some considerations on explicit damage models including crack closure effects and anisotropic behaviour, *Proceedings FRAMCOS-2*, Ed.F.H. Wittmann, AEDIFICATIO Publisher, Freiburg.
- Rouquand A., 2005, Presentation d'un modèle de comportement des géomatériaux, applications au calcul de structures et aux effets des armes conventionnelles, Centre d'Etudes de Gramat, rapport technique T2005-00021/CEG/NC.
- Van Mier J.G., Pruijssers A., Reinhardt H.W., Monnier T., 1991, Load time response of colliding concrete bodies, *J. of Structure Engineering*, vol. 117, p. 354-374.